Diamonds in Dense Molecular Clouds: A Challenge to the Standard Interstellar Medium Paradigm

L. J. Allamandola,* S. A. Sandford, A. G. G. M. Tielens,
T. M. Herbst

Observations of a newly discovered infrared C–H stretching band indicate that interstellar diamond-like material appears to be characteristic of dense clouds. In sharp contrast, the spectral signature of dust in the diffuse interstellar medium is dominated by $-CH_2-$ and $-CH_3$ groups. This dichotomy in the aliphatic organic component between the dense and diffuse media challenges standard assumptions about the processes occurring in, and interactions between, these two media. The ubiquity of this interstellar diamond-like material rules out models for meteoritic diamond formation in unusual circumstellar environments and implies that the formation of the diamond-like material is associated with common interstellar processes or stellar types.

Weak infrared absorptions characteristic of the C–H stretching vibrations of the carbonaceous component of interstellar dust and ices have long been expected to be present in the spectra of dense molecular clouds. A high-resolution spectral study of these features is important because peak frequencies and relative strengths are characteristic of specific molecules and chemical classes, and such a study has the potential to reveal much about the composition of the dust.

The infrared spectra of protostars embedded in dense interstellar clouds generally show deep ice absorption features (*1–3*). We recently obtained high-resolution (2.5 cm^{-1}) spectra of four protostars in the C–H stretching region from 3100 to 2600 cm^{-1} (3.2 to 3.9 μm) in order to classify and quantify the hydrocarbon components of dense clouds. Besides the C–H stretch of methanol ice at 2825 cm^{-1} in two of the spectra, the spectra of all four objects also revealed an absorption feature centered at ~2880 cm^{-1} (full width at half maximum height ≈ 90 cm^{-1}) (*4*) (Fig. 1).

This band occupies a unique position in the aliphatic C–H stretch region. Absorptions falling within 15 cm^{-1} of 2890 cm^{-1} (3.46 μm) are characteristic of stretching vibrations of tertiary CH:

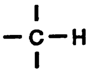

$$-\overset{|}{\underset{|}{C}}-H$$

A tertiary aliphatic C atom is one in which three of its four single (sp^3) bonds are to other C atoms; the remaining bond is to a different species, such as hydrogen (*5*). Absorptions due to $-CH_3$ and $-CH_2-$ groups fall shortward and longward of 2880 cm^{-1} (*6, 7*). Thus, we attribute the 2880-cm^{-1} band to the tertiary CH group (*4*). Because the integrated absorbances per C–H bond are comparable for $-CH_3$, $-CH_2-$, and tertiary CH (*8*), the predominance of the 2880-cm^{-1} (3.47 μm) band places significant constraints on the structure of this hydrocarbon. If there were equal numbers of each type of hydrogenated C atom in the interstellar material, there would be prominent bands at ~2960 cm^{-1} ($-CH_3$) and 2925 cm^{-1} ($-CH_2-$), a moderate band at 2880 cm^{-1} (tertiary CH), and weak to moderate features at 2870 cm^{-1} ($-CH_3$) and 2860 cm^{-1} (tertiary CH). This is not the case (Fig. 1). Instead the spectrum shows that tertiary CH groups are more abundant than $-CH_2-$ and $-CH_3$ groups in dense molecular clouds by factors of at least 3 and 10, respectively. The smallest molecular structure that satisfies the $CH:CH_2:CH_3$ = 10:3:1 requirement consists of a three-dimensional cluster containing more than 30 sp^3-bonded, interconnected C atoms with the surface atoms bonded to H atoms. This is the diamond structure of C. Realizing that one infrared band is generally insufficient for a secure assignment, we tentatively attribute this new feature to interstellar "microdiamonds" because of its spectral position and predominance, in conjunction with the lack of other aliphatic bands.

The optical depth of the 2880-cm^{-1} band toward the protostar NGC 7538 IRS 9 (Fig. 1) places a lower limit of ~5% on the amount of cosmic C in the material (*4*). This is only a lower limit because it considers only those tertiary C atoms that are bound to H. Additional skeletal C atoms must also be associated with this diamond-like material, as well as C in nonhydrogenated π-bonded surface atoms and in $-CH_3$ and $-CH_2-$ groups. If $-CH_3$ and $-CH_2-$ groups are responsible for all the absorption at 2960 and 2925 cm^{-1} in Fig. 1, the additional C content in these groups would be as much as 40% of the measured tertiary C abundance.

If there is a connection between the carrier of the band we observed and the interstellar microdiamonds found in meteorites (*9–11*), additional constraints can be placed on the amount of cosmic C tied up in the interstellar carrier. Electron-energy loss spectra show that the meteoritic diamonds contain mainly sp^3 C–C bonds with some π-type (sp^2) C=C bonds (*9–11*). The relatively constant ratio of the π-bonded (sp^2) C to σ-bonded (sp^3) C in meteoritic diamonds has been taken to imply that the π-bonded C is part of the surface (*11*). If we assume that the interstellar diamonds have the same surface properties and size distribution as those of the meteoritic diamonds, then for every tertiary CH we detect, there could be as many as three additional C atoms bound only to other skeletal C atoms. Considering these possibilities, the tertiary CH abundance could be an underestimate of the total C abundance of this carrier by a factor of as much as 4; thus, 10 to 20% of cosmic C could be associated with the 2880-cm^{-1} band carrier. This compares with 10 to 20% in the form of CO, 10 to 50% in CH_3OH, 10% in polycyclic aromatic hydrocarbons, and about 25% thought to be in amorphous C. This 10 to 20% abundance in microdiamonds is similar to the amount predicted to be pro-

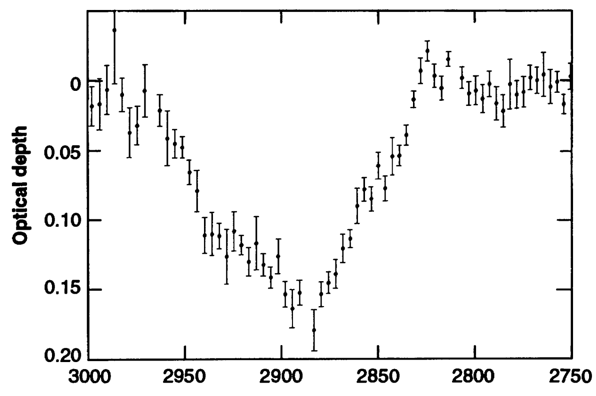

Fig. 1. The interstellar 2880-cm^{-1} band of NGC 7538 IRS 9 assigned principally to the tertiary CH stretch of diamond-like C in dense molecular clouds. This is the residual spectrum obtained after removal of the local continuum and the solid methanol feature for the source with the best defined 2880-cm^{-1} feature, NGC 7538 IRS 9. See (*4*) for details and the spectra of the protostars W33A, S140, and W3 IRS5.

L. J. Allamandola, S. A. Sandford, A. G. G. M. Tielens, National Aeronautics and Space Administration, Ames Research Center, Mail Stop 245-6, Mountain View, CA 94035.
T. M. Herbst, Institute for Astronomy, 2680 Woodlawn Drive, University of Hawaii, Honolulu, HI 96822.

---

*To whom correspondence should be addressed.

duced by shock waves in the interstellar medium (ISM) (*12*) and is consistent with the suggestion that microdiamonds should be stable in space (*13*) while graphite may be rare (*14*). This range is also similar to the 25% value for all (including aliphatics) of the *sp*^{3} carbon proposed to be associated with amorphous carbon particles, suggesting that interstellar amorphous C may be associated with the microdiamonds (*15*).

The present observations also bear on questions concerning the origin of interstellar microdiamonds recovered from meteorites. These diamonds contain nonsolar isotopic abundances of Xe, Ne, N, and H, indicating an interstellar origin (*16*). In contrast to the prominence of the tertiary CH feature (2880 cm^{-1}) in the interstellar spectra, the infrared spectra of meteoritic microdiamonds are dominated by $-CH_3$ and $-CH_2-$ bands in the aliphatic C–H stretch region (*10*). These meteoritic $-CH_3$ and $-CH_2-$ groups could result from hydrogenation of surface sites during the extensive chemical processing required to separate the microdiamonds from the other meteoritic components. Similarly, surface-modifying effects are also expected for naturally occurring and industrial-grade synthetic diamonds (*17, 18*). The predominance of the tertiary CH feature in the interstellar spectra emphasizes the unique character of the interstellar diamond-like material observed in dense clouds.

Our detection of the 2880-cm^{-1} band in all four of the dense clouds that we studied indicates that interstellar diamond-like material is abundant and ubiquitous in the interstellar medium. Thus, hypotheses that attempt to explain the isotopic anomalies by invoking rare formation sites for the meteoritic diamonds (*19, 20*) can be excluded on the basis of abundance considerations. This conclusion is also supported by the almost solar $^{12}C/^{13}C$ ratios found in meteoritic diamonds. Both ^{12}C and ^{13}C are injected into the ISM by many different stellar sources, each characterized by a nonterrestrial $^{12}C/^{13}C$ ratio (*21*). The nearly solar $^{12}C/^{13}C$ ratio of meteoritic diamonds ($^{12}C/^{13}C \sim 89$) is difficult to reconcile with an origin in a single type of stellar source. In contrast, highly anomalous $^{12}C/^{13}C$ ratios have been measured in SiC grains isolated from meteorites. These grains, because of this anomaly and other s-process (a type of nucleosynthetic pathway) abundance anomalies, are thought to have originated only from C-rich giants. Although the measured Xe anomalies in meteoritic diamonds are at variance with the arguments against a diamond origin from rare stellar sites, only 1 in 10^6 diamonds needs to contain a Xe atom in order to account for the Xe abundances. The possibility that a small contribution of diamond stardust from type II supernovae is responsible for the Xe anomaly is not excluded by our observations.

The infrared spectrum (in the C–H stretch region) of dust in the diffuse ISM is dramatically different from the spectrum of dust in the dense medium (Fig. 2). The hydrocarbon dust component of the diffuse ISM contains aliphatic hydrocarbons rich in methyl ($-CH_3$) and methylene ($-CH_2-$) groups in a ratio ~2.5:1 (*22*). These are present as short chains, two to three C atoms long, attached to perturbing electronegative groups such as OH. The spectra of the diffuse ISM material suggest that it is similar to meteoritic kerogen (*23, 24*). Thus, it appears that diamond-like material is ubiquitous in dense clouds whereas methyl- and methylene-rich material is dominant in the diffuse ISM. This difference, which does not depend on the actual carrier of the 2880-cm^{-1} band, is surprising in view of the thorough mixing expected between the dense and diffuse media.

It is difficult to understand the absence of the $-CH_2-$ and $-CH_3$ bands in the spectra of embedded protostars. The following illustrates the remarkable extent of this bifurcation of hydrocarbons between the dense and diffuse media. If we scale by the visual extinction (A_v), a measure of the total amount of material present, the C–H stretching band observed toward Galactic Center source IRS 7 (which primarily samples diffuse ISM dust) to that of NGC 7538 IRS 9 (which primarily samples dense ISM dust), a feature with a peak optical depth of about 0.6 at 2960 cm^{-1} would be expected in the spectrum of NGC 7538 IRS 9. This is three times the depth of the new interstellar band at 2880 cm^{-1} shown in Fig. 1. Indeed, if it were present, it would likely obscure the 2880-cm^{-1} feature. Its absence implies that C-rich materials in the diffuse medium do not become incorporated into, or do not survive incorporation into, dense molecular clouds. Neither destruction by shocks (which are weak in dense clouds), nor ultraviolet photolysis (mild as a result of dust extinction), nor H-atom attack (which would make $-CH_3$ and $-CH_2-$ groups rather than destroy them) can explain the apparent lack of the C-rich diffuse-cloud component in dense clouds.

Various explanations have been proposed to explain the aliphatic C associated with the features of the diffuse ISM, including direct deposition of hydrogenated amorphous C films (*25*) and ultraviolet photolysis of ice mantles in dense clouds (*22, 26, 27*). In view of the expected fast exchange of material between the diffuse and dense media (*28*) and the rather benign conditions in dense clouds as compared to those in the diffuse ISM, the predominance of the 2880-cm^{-1} signature and the absence of clear $-CH_3$ and $-CH_2-$ absorption features in the dense medium are puzzling. This conclusion is independent of the identity of the 2880-cm^{-1} interstellar absorption band carrier.

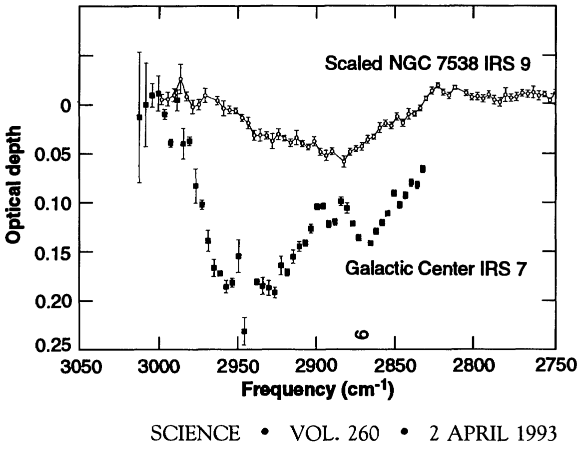

Fig. 2. The spectra, in the C–H stretch region, of NGC 7538 IRS 9 (representative of dust in the dense ISM) and of Galactic Center source IRS 7 (characteristic of dust in the diffuse ISM). The spectrum of NGC 7538 IRS 9 has been scaled to match an A_v equivalent to that toward the galactic center. This comparison illustrates the unexpected, fundamental differences between the refractory aliphatic organics in the two media.

REFERENCES AND NOTES

1. S. P. Willner *et al.*, *Astrophys. J.* **253**, 174 (1982).
2. A. G. G. M. Tielens and L. J. Allamandola, in *Physical Processes in Interstellar Clouds*, G. E. Morfill and M. Scholer, Eds. (Reidel, Dordrecht, Holland, 1987), p. 333.
3. A. G. G. M. Tielens, in *Interstellar Dust*, L. J. Allamandola and A. G. G. M. Tielens, Eds. (Kluwer, Dordrecht, Holland, 1989), p. 239.
4. L. J. Allamandola, S. A. Sandford, A. G. G. M. Tielens, T. Herbst, *Astrophys. J.* **399**, 134 (1992).
5. R. T. Morrison and R. N. Boyd, *Organic Chemistry* (Allyn and Bacon, Boston, 1966).
6. L. J. Bellamy, *The Infra-Red Spectra of Complex Organic Molecules* (Wiley, New York, ed. 2, 1958).
7. R. M. Silverstein and G. C. Bassler, *Spectrometric Identification of Organic Compounds* (Wiley, New York, 1967), chap. 3.
8. A. S. Wexler, *Appl. Spectrosc. Rev.* 1, 29 (1967).
9. D. F. Blake *et al.*, *Nature* **332**, 611 (1988).
10. R. S. Lewis, E. Anders, B. T. Draine, *ibid.* **339**, 117 (1989).
11. T. J. Bernatowicz, P. C. Gibbons, R. S. Lewis, *Astrophys. J.* **359**, 246 (1990).
12. A. G. G. M. Tielens, C. G. Seab, D. J. Hollenbach, C. F. McKee, *ibid.* **319**, L109 (1987).
13. J. A. Nuth III, *Nature* **329**, 589 (1987).
14. ———, *ibid.* **318**, 166 (1985).
15. A. P. Jones, W. W. Duley, D. A. Williams, *Q. J. R. Astron. Soc.* **31**, 567 (1990).
16. R. S. Lewis, M. Tang, J. F. Wacker, E. Anders, E. Steel, *Nature* **326**, 160 (1987); M. Tang and E. Anders, *Geochim. Cosmochim. Acta* **52**, 1235 (1988).
17. K. Kobashi *et al.*, *SPIE* **969**, 159 (1988).

18. G. S. Sandhu, W. K. Chu, M. L. Swanson, J. F. Prins, *ibid.*, p. 37.
19. D. D. Clayton, *Proc. Lunar Planet. Sci. Conf.* **12B**, 1781 (1981).
20. U. G. Jorgenson, *Nature* **332**, 702 (1988).
21. A. G. G. M. Tielens, in *Carbon in the Galaxy: Studies from Earth and Space* (National Aeronautics and Space Administration Publication CP-3061, Washington, DC, 1990), p. 59.
22. S. A. Sandford *et al.*, *Astrophys. J.* **371**, 607 (1991).
23. P. Ehrenfreund, F. Robert, L. d'Hendecourt, F. Behar, *Astron. Astrophys.* **252**, 612 (1992).
24. Y. Pendleton, S. A. Sandford, L. J. Allamandola, A. G. G. M. Tielens, K. Sellgren, in preparation.
25. W. W. Duley, A. P. Jones, D. A. Williams, *Mon. Not. R. Astron. Soc.* **236**, 709 (1989).
26. J. M. Greenberg, in *Submillimeter Wave Astronomy*, J. E. Beckman and J. P. Phillips, Eds. (Cambridge Univ. Press, Cambridge, 1982), p. 261.
27. L. J. Allamandola, S. A. Sandford, G. J. Valero, *Icarus* **76**, 225 (1988).
28. C. F. McKee, in *Interstellar Dust*, L. J. Allamandola and A. G. G. M. Tielens, Eds. (Kluwer, Dordrecht, Holland, 1989), p. 431.
29. We thank E. Anders and R. Lewis for discussion concerning the connections between the interstellar diamond band and meteoritic microdiamonds. This work was supported by National Aeronautics and Space Administration grants 199-52-12-04 and 452-33-93-03.

13 November 1992; accepted 21 January 1993

Strong, Pure, and Uniform Carbon Fibers Obtained Directly from the Vapor Phase

Frederick T. Wallenberger and Paul C. Nordine

With laser-assisted chemical vapor deposition, strong and flexible carbon fibers were obtained at high reaction chamber pressures (>1 bar) with growth rates >0.3 millimeter per second; their tensile strength (3 gigapascals) approaches that of commercial intermediate modulus carbon fibers made by conventional process routes. With the process described here, carbon fibers can be produced with superior chemical purity and structural uniformity. They may become the material of choice in currently emerging premium end uses, including carbon fiber infrared detection elements.

In 1972, Nelson and Richardson (*1*) were able to fabricate short carbon rods from methane and ethane with diameters >200 μm by laser-assisted chemical vapor deposition (LCVD) using a CO_2 laser and low reaction chamber pressures (<1 bar). Their process, which used laser heating of the growing fiber tip as the heat source to decompose the gaseous reactants, was slow (<10 μm s^{-1}); the carbon rods were weak and brittle because of considerable structural nonuniformities. Between 1981 and 1988, Bäuerle and others (*2*) made short carbon fibers from methane, ethylene, and acetylene by a similar LCVD process. Using an efficient Ar^+ laser, they obtained small fiber diameters (<25 μm), but because they also used low reaction pressures (<1 bar) they too obtained low growth rates (<20 μm s^{-1}).

In 1992, Westberg *et al.* (*3*) documented the structural complexity of small diameter carbon lines (<20 μm) that had been deposited from ethylene by a low-pressure LCVD process (<1 bar) under hot- and cold-wall conditions like those reported by Bäuerle (*2*). As shown with scanning electron microscopy (SEM) (*3*), a hot-wall material, for example, had a relatively smooth but nodular surface. Cleavage, however, showed that it had a layered and perhaps brittle core structure. Short carbon fibers were recently also obtained by metal- (versus laser-) catalyzed vapor deposition with a hot metal particle as the heat source to decompose hydrogen-hydrocarbon gases (*4*). Cylindrical hollow-core fibers result that are not visible with optical microscopy. They can be thickened and lengthened by further vapor deposition. Lengthening ceases when a metal particle is covered by pyrolytic carbon. The best summary of this technology, which yields structurally complex materials, is found in a recent review article by Tibbetts (*4*). Here, we describe the fabrication of highly uniform carbon fibers by LCVD with up to 30 times the previously documented (*1–3*) growth rates and tensile strength values that approach those of commercial intermediate modulus (IM) carbon fibers. This result was made possible through the use of an LCVD process with a reaction pressure >1 bar.

Laser-assisted chemical vapor deposition uses the focal point of a laser beam as the heat source to decompose the gaseous reactants rather than a hot reaction chamber or a hot substrate surface, as in a conventional chemical vapor deposition process. For our experiments, reaction pressures >1 bar were used. Figure 1 shows the LCVD growth of a fiber with time. Under these conditions, the hot focal point of the laser is continually adjusted in the reaction chamber (Fig. 2) to coincide with the tip of the growing fiber and to support the continuous growth of fibers directly from the vapor phase. The fabrication of microsprings and microsolenoids was recently viewed (*5*) as well as the formation of strong, small-diameter boron fibers (*6*).

The experimental apparatus (*6*) for growing the carbon fibers consisted of an optical bench with a continuous 5-W Nd–yttrium-aluminum-garnet (YAG) laser, a small reaction chamber in an enclosed laboratory hood, a system for delivering the feed gases, a microscope attached to the reaction chamber to observe and record the growth of individual fibers, and computer-operated laser power controls and stepper motors to drive the fiber pulling rate. The fiber diameters that were achieved in this process are nearly equal to the diffraction-limited laser focal spot size. The size of laser focal spot, in turn, depends on the wavelength of the laser. A small reaction chamber served as a research tool. It is suitable for producing, side-by-side, several 1.4-cm-long fiber specimens along the edge of a common substrate, a carbonized cardboard. The diameters of high-pressure–LCVD (HP-LCVD) carbon fibers made so far range from less than 10 μm to more than 30 μm.

In this apparatus, any process variable (such as pressure, feed rate, or pulling rate) can be changed within minutes, while all the others are kept constant. A simple modification of this chamber facilitates the growth of fibers up to 2 m long and the growth of potentially endless fibers directly from the vapor phase. In our experiments, carbon fibers were grown from methane and from ethylene. When grown from methane, the reactant pressures ranged from 3.4 to >7.1 bar. Individual fibers grew at a rate ranging from 9 to 331 μm s^{-1} and with diameters ranging from 20 to 170 μm. Much smaller diameter fibers may be grown at reduced laser power and increased reactor pressure. The fibers grown from ethylene

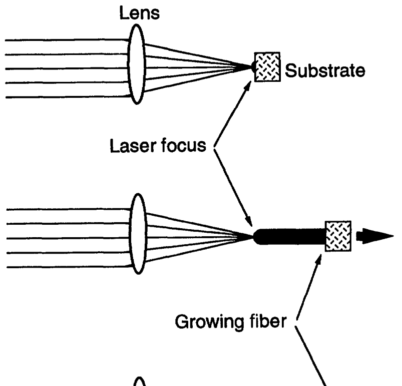

Fig. 1. Fiber growth by LCVD.

F. T. Wallenberger, Department of Materials Science and Engineering, University of Illinois, 1304 West Green Street, Urbana, IL 61801.
P. C. Nordine, Containerless Research Incorporated, 735 Carriage Way, Deerfield, IL 60015.